



## Well Logs and Petrophysical Characteristics of the Hartha Formation at Balad Oil Field, Central Iraq

Lina M. Salman<sup>1\*</sup> , Sawsan H. Alhazaa<sup>2</sup> 

<sup>1,2</sup> Department of Applied Geology, College of Science, University of Tikrit, Tikrit, Iraq.

### Article information

**Received:** 22- Mar -2024

**Revised:** 15- May -2024

**Accepted:** 03- June -2024

**Available online:** 01- Apr – 2025

#### Keywords:

Hartha Formation

Well logs

Petrophysical Properties

CPI

M-N cross-plot

### ABSTRACT

The Hartha Formation is a crucial oil production reservoir in southern and central Iraq; known for its diverse carbonate sediments. The Hartha Formation at Balad oil field is divided into upper and lower parts. Based on the petrophysical characteristics (resistivity, porosity, and saturation), the lower parts of the Hartha Formation that contain the hydrocarbons are divided into two units: Har.UA and Har. UB. Analysis using the M-N cross-plot showed that calcite is the predominant mineral in the Hartha Formation, with dolomite and shale occurring to a lesser extent. Additionally, the neutron vs. density cross-plot analysis reveals that the Hartha Formation is primarily composed of limestone with dolomite as a secondary component. Based on the ComputerProcessing Interpretation (CPI) analysis of five wells studied at the Balad oil field, the wells in the northeastern block (Ba-5, Ba-6, and Ba-7) exhibit favorable reservoir quality. These wells are characterized by higher porosity fractions (0.228, 0.215, and 0.224), lower water saturation fractions (0.093, 0.099, and 0.092), and higher hydrocarbon saturation fractions (0.906, 0.9004, 0.907). Based on the separation of neutron and density records, these wells contain oil and gas phases, especially wells (Ba-6 and Ba-7). On the other hand, the wells located in the graben area (Ba-1 and Ba-8) demonstrate lower reservoir quality with porosity fractions of (0.13 and 0.20), water saturation fractions of (0.347 and 0.257), and hydrocarbon saturation fractions of (0.652 and 0.708), show only a single phase, specifically an oil zone.

#### Correspondence:

**Name:** Lina M. Salman

**Email:** [leenasalman444@gmail.com](mailto:leenasalman444@gmail.com)

DOI: [10.33899/earth.2024.146871.1230](https://doi.org/10.33899/earth.2024.146871.1230), ©Authors, 2025, College of Science,, University of Mosul.

This is an open-access article under the CC BY 4.0 license (<http://creativecommons.org/licenses/by/4.0/>) .

# المجسات البئرية والخصائص البتروفيزيائية لتكوين هارثه في حقل بلد النفط، وسط العراق

لينا مولود سلمان <sup>1\*</sup> ID ، سوسن حميد الهزاع <sup>2</sup> ID

<sup>1,2</sup> قسم علم الارض التطبيقية ، كلية العلوم، جامعة تكريت، تكريت، العراق.

المخلص	معلومات الارشفة
يعد تكوين هارثه من المكامن المهمة والمنتجة للنفوط في جنوب ووسط العراق وهو ذو رواسب كاربوناتية مختلفة . قسم تكوين هارثه في حقل بلد الى جزء علوي وجزء سفلي. بناءً على الخصائص البتروفيزيائية (المقاومية، المسامية، والتشبع)، تم تقسيم الأجزاء السفلية من تكوين هارثه التي تحتوي على الهيدروكربون إلى وحدتين: Har.UA و Har.UB . يشير التحليل باستخدام مخطط M-N إلى أن الكالسيت هو المعدن السائد في تكوين هارثه، مع وجود الدولوميت والسجيل بدرجة أقل. بينت نتائج التحليل المتقاطع للنيوترون مقابل الكثافة أن تكوين هارثه يتكون بشكل أساسي من الحجر الجيري، مع الدولوميت كمكون ثانوي. استناداً إلى نتائج تفسير المعالجة الحاسوبية (CPI) لخمسة آبار تمت دراستها في حقل بلد النفط، تظهر الآبار الموجودة في القطاع الشمالي الشرقي ( Ba-5 ، Ba-6 ، و Ba-7) جودة مكمية مناسبة. وتتميز هذه الآبار بمساميتها العالية (0.228 و 0.215 و 0.224) وانخفاض تشبعها بالماء (0.093 و 0.099 و 0.092) وارتفاع تشبعها بالهيدروكربون (0.906 و 0.9004 و 0.907). وبناءً على فصل سجلات النيوترونات والكثافة، فإن هذه الآبار تحتوي على طوري النفط والغاز وبالأخص بنرا (Ba-6) و (Ba-7). من ناحية أخرى، فإن الآبار الموجودة في منطقة الحوض (Ba-1) و (Ba-8) تظهر انخفاض جودة الخزان مع نسبة مسامية تبلغ (0.13 و 0.20) ونسبة تشبع مائي (0.347 و 0.257) ونسبة تشبع هيدروكربوني (0.652 و 0.708) ، كما انها تحتوي على النفط فقط.	تاريخ الاستلام: 22- مارس -2024 تاريخ المراجعة: 15- مايو -2024 تاريخ القبول: 03- يونيو -2024 تاريخ النشر الإلكتروني: 01- ابريل -2025 الكلمات المفتاحية: تكوين الهارثه المجسات البئرية الخصائص البتروفيزيائية المعالجة الحاسوبية مخطط M-N المراسلة: الاسم: لينا مولود سلمان Email:leenasalman444@gmail.com

DOI: [10.33899/earth.2024.146871.1230](https://doi.org/10.33899/earth.2024.146871.1230), ©Authors, 2025, College of Science., University of Mosul.

This is an open-access article under the CC BY 4.0 license (<http://creativecommons.org/licenses/by/4.0/>) .

## Introduction

The Hartha Formation serves as a substantial reservoir for oil production in south and central Iraq, consisting of a heterogeneous carbonate composition. This formation primarily consists of neritic carbonate sediments that belong to the Late Turonian-Danian Megasequence AP9 within the Late Campanian-Maastrichtian sequence (Buday,1980). The initial discovery of the Hartha Formation took place in well Zubair-3 located in southern Iraq, and identified by Rabanit in 1952 (Owen and Nasr, 1958). It was deposited during the Upper Campanian-Lower Maastrichtian sequence, in carbonate inner shelf and lagoonal back reef environments surrounding the stable shelf margins (Jassim and Goff, 2006). The Balad oil field, our focal point, is situated between the Samara Field in the north and the east Baghdad Field in the south (Fig. 1). The field experienced two major faults and many minor faults that divided the Hartha Formation at the Balad oil field into three main zones, including the northeastern shoulder, graben, and southwestern shoulder. These faults are longitudinal normal faults that extend over 20 km and follow the northwest-southeast trending extension (Al-Naemi, 2012).

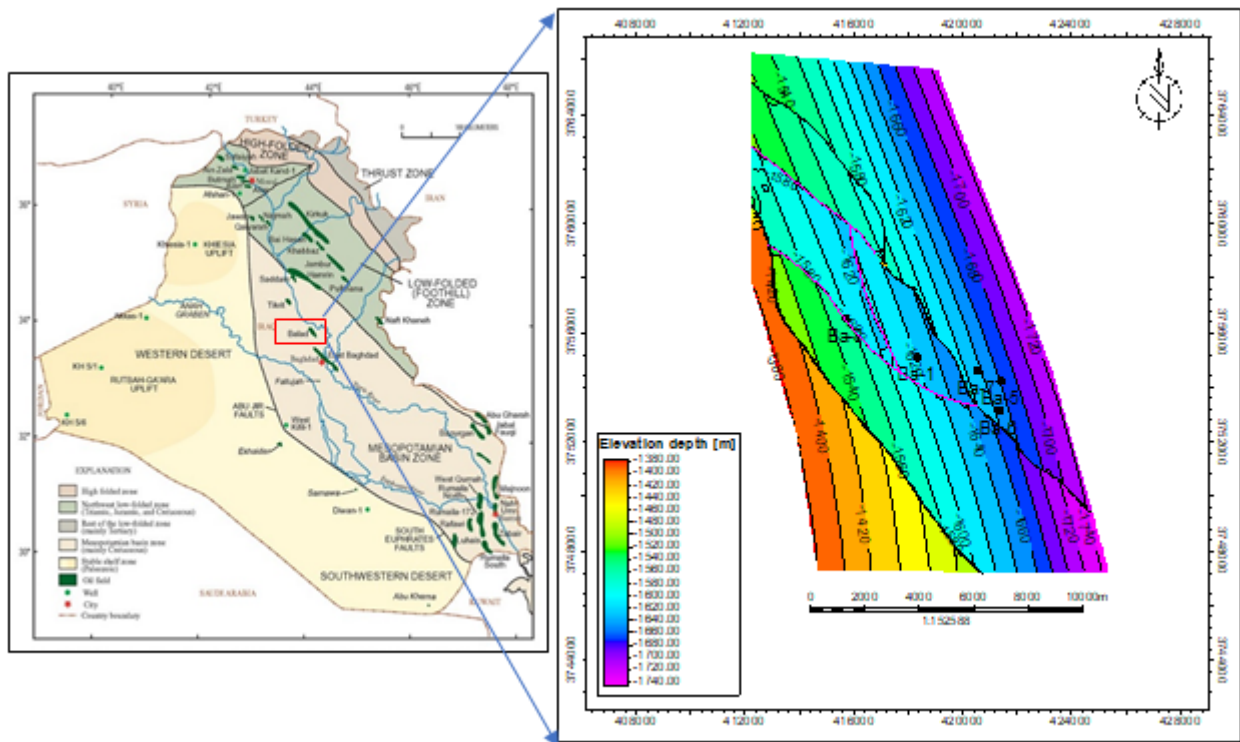


**Fig. 1. Location and structural contour map of Hartha Formation in the study area modified from Al-Naemi (2012).**

The Balad oil field is positioned within the unstable shelf of the Arabian platform, as per the geosyncline theory outlined by Buday and Jassim (1987). Numan (1997) divided Iraq's plate tectonics into seven main sections using plate tectonic theory. According to these divisions, the study area falls inside the sagged basins of the Mesopotamian Zone in the quasipatform foreland belt. Fauad (2010) redefined the Mesopotamian Zone as the Mesopotamian foredeep, aligning with the current understanding of foreland basins. The Mesopotamian foredeep contains several subsurface folds and faults covered with Quaternary sediments. The general trend of these folds is E-W in the northwestern part and NW-SE in other parts of the Mesopotamian foredeep. The faults, on the other hand, can be categorized as normal faults, following two main trends: NW-SE and ENE-WSW. According to drilling reports provided by North Oil Company (NOC, 1984), the Hartha Formation at Balad oil field is primarily composed of two parts. The upper part consists of limestone, argillaceous in parts, marly in parts, pyritic, chalky limestone, dolomitic, and fossiliferous. The lower part comprises limestone, finely crystalline, porous impregnated with heavy oil, pyritic, shaly in parts, stylolites, and locally dolomitized. The lower part, which contains the oil, can be further divided into two units (A and B) based on well logs and petrophysical properties (Fig. 2). The upper boundary of the Hartha Formation conforms with the overlying pelagic sediments of the Shiranish Formation (Jassim and Goff 2006). Conversely, the lower boundary is typically discordant with the Mushorah Formation, often indicating a missing Middle-Campanian period (Haq et al., 1987). The thickness of the Hartha Formation at the Balad oil field varies owing to the presence of faults, ranging from 292 m in well Ba-5 to 444 m in well Ba-1.

### **Aim of study**

This paper emphasizes the petrophysical assessment of the Hartha Formation using a set of open-hole logs obtained from 5 wells (Ba-1, 5,6,7, and 8) within the Balad oil field. These logs include GR, Caliper, porosity logs- and resistivity logs.

## Materials and Methods

The petrophysical analysis is achieved in two major steps: the first, is done via digitizing some of the available well log data by using NeuraLog software V.15.4. The second, represents the Computer Processing Interpretation (CPI) of open hole logs including GR, Caliper, porosity logs- and resistivity logs data using Techlog software V.15.3. It is important to note that the well-log data received from the North Oil Company only covers the lower part of the Hartha Formation that comprises the hydrocarbons, except for Ba-1, and the resistivity logs data was collected and digitized as provided by Al-Sammarai's (2010) thesis.

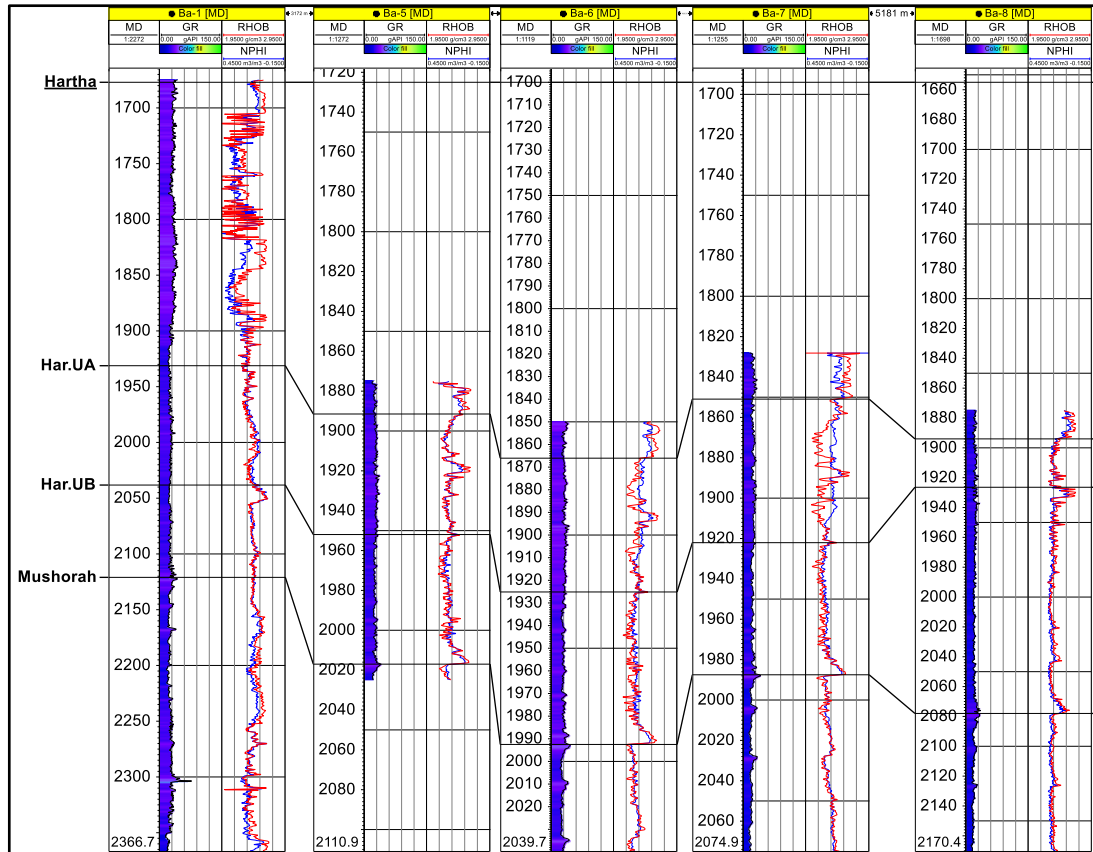


Fig. 2. Hartha Formation thickness of five selected wells at Balad oil field.

## Results and Discussion

### Porosity Logs

Porosity is defined as the ratio of pore space within a rock to the total volume of that rock, which is an important characteristic of all reservoir types. The porosity is also defined as the storage capacity of the sedimentary rock for oil, gas, and water (Lucia et al., 2003). In reservoir rocks, porosity is categorized into absolute porosity (total porosity) encompassing connected and non-connected pores, and effective porosity which includes the interconnected pore space that can transmit the fluid (Inteq, 1992). The porosity can be assessed directly from the core or indirectly from the well logs (Selley, 1998, Cheng et al., 2023). In this study, the porosity is calculated using three well logs tools including density, neutron, and sonic. As displayed in CPI figures (7 to 11).

#### 1. Density log

Bulk density refers to the overall density of both solids and fluid components within a rock formation (Gadekea et al., 1988). It is typically measured in grams per cubic centimeter (g/cc) and has various applications, including porosity calculation, detection of gas-bearing formation, identification of evaporites, and determination of lithology with the neutron log

(Inteq,1992). The porosity derived from the density log represents total porosity and can be calculated using the equation provided by Asquith and Krygowski (2004).

$$\phi_D = \frac{(\rho_{ma} - \rho_b)}{(\rho_{ma} - \rho_f)} \quad (1)$$

where,  $\phi_D$  = density-derived porosity,  $\rho_b$  = log reading bulk density,  $\rho_{ma}$  = dry rock density for limestone,  $\rho_f$  = fluid density for oil.

## 2. Neutron Log

The neutron log assesses the hydrogen concentration present in the porous formation based on the collision speed between neutron and hydrogen particles within the formation (Schlumberger, 1998). It is utilized for detecting porosity, gas-bearing zones (not liquid-filled), and lithology identification. The combination of neutron logs with density logs can provide a more accurate calculation for total porosity determination (Schlumberger, 1972). In this study, the formula used to estimate the total porosity of the Hartha Formation as shown in (Fig. 3) is as follows:

$$\Phi_t = \phi_N + \phi_D/2 \quad (2)$$

where,  $\Phi_t$  = porosity of neutron and density,  $\phi_N$  = neutron porosity,  $\phi_D$  = density porosity.

## 3. Sonic Log

The sonic log provides a continuous recording of the interval transit time ( $\Delta t$ ) versus the depth of the acoustic wave traveling through the formation along the wellbore axis. The transit time is influenced by the lithology type and porosity (Selley, 1998). The porosity derived from the sonic log represents primary porosity formed during deposition and can be estimated using the following formula:

$$\phi_S = \frac{(\Delta t - \Delta t_{ma})}{(\Delta t_f - \Delta t_{ma})} \quad (3)$$

where,  $\phi_S$  = sonic porosity,  $\Delta t$  = interval transit time of formation (recorded by log),  $\Delta t_f$  = interval transit time in fluid (oil),  $\Delta t_{ma}$  = interval transit time of matrix (limestone).

## 4. Primary and Secondary porosity

The primary porosity is the original porosity existing in the rock formations during deposition and lithification (Cheng et al., 2023). The primary porosity may have various forms depending on how the formations were acutely deposited (Schlumberger, 1989). The intragranular and intergranular porosities are the most common primary porosity that can be detected by sonic logs (Asquith and Gibson, 1982). In contrast, secondary porosity is formed through rock alterations, such as dolomitization, dissolution, and fracturing (Prather et al., 2023). This type of porosity can also result from water and tectonic forces acting on the rock matrix post-deposition (Tiab and Donaldson, 2015). The secondary porosity has many forms depending on the geological processes such as vugs, moldic, channel, and fracture. The caliper log readings at the well (Ba\_1) are notably high, which affected the accuracy of porosity calculations using the neutron and density logs. Consequently, porosity is assessed using the sonic log, while the estimation of secondary porosity is not possible due to the impact of washout in the wellbore. According to Schlumberger (1997), the formula provided can be used to estimate the secondary porosity as shown in Figure (3) is.

$$SPI = (\Phi_t - \phi_S) \quad (4)$$

where,  $SPI$  = index of secondary porosity,  $\Phi_t$  = porosity of neutron–density,  $\phi_S$  = porosity of sonic

### 5. Effective porosity

The effective porosity is the proportion of interconnected spaces within a rock to its total volume, playing a vital role in determining the fluid capacity of these voids. According to Schlumberger (1998), the effective porosity can be calculated using the equation provided, as revealed in (Fig. 3).

$$\Phi_e = \Phi_t \times (1 - VSh) \quad (5)$$

where,  $\Phi_e$  = effective porosity,  $\Phi_t$  = total porosity,  $VSh$  = shale volume

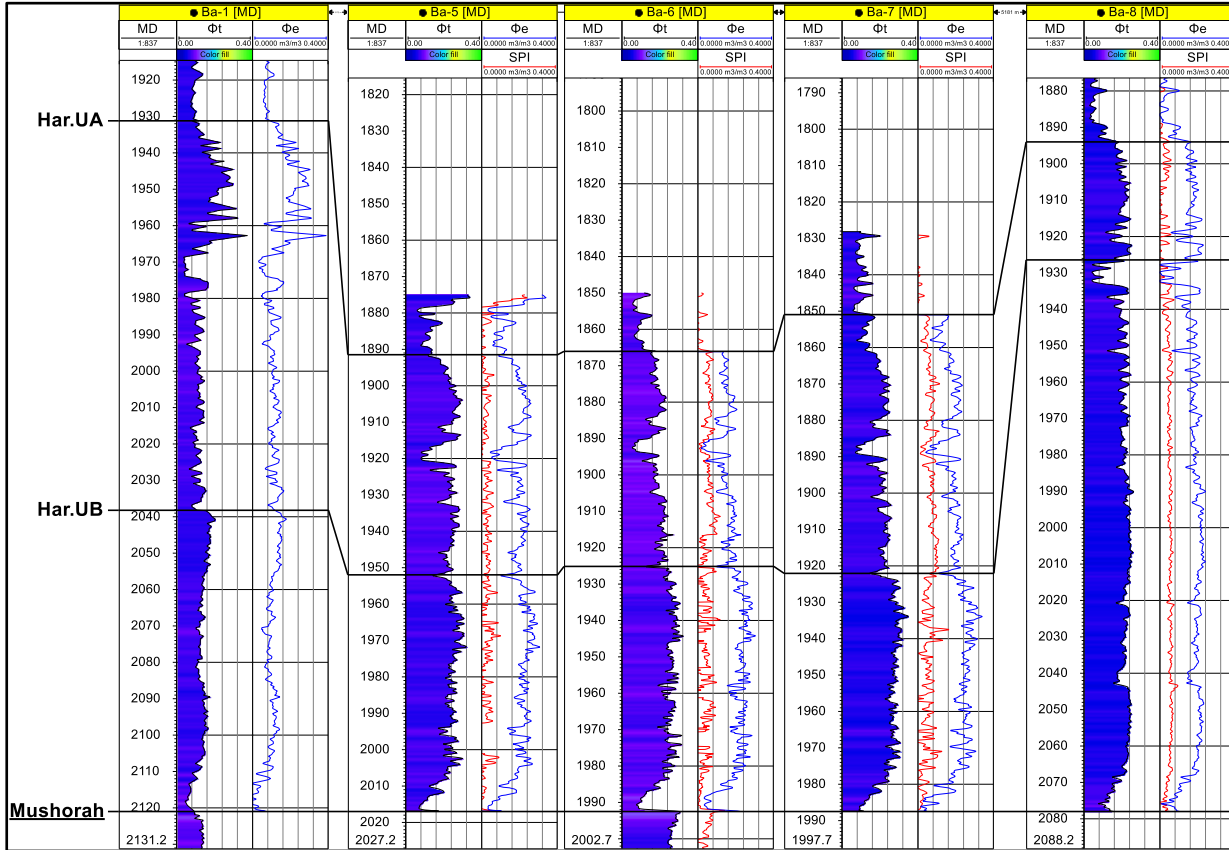


Fig. 3. The distribution of total porosity, effective porosity, and secondary porosity of Hartha units (A and B) for five studied wells at Balad oil field.

### Determination of Mineralogy and Lithology

The mineralogy and lithology of the Hartha Formation are identified by analyzing three sets of porosity logs - density, neutron, and sonic - within the Techlog software.

#### 1. M-N Cross Plot for Mineral Identification

The M-N cross plot used the density, neutron, and sonic to detect the binary and ternary of complex minerals mixtures such as (calcite, dolomite, anhydrite, quartz, etc). Schlumberger (1979) provides a formula for estimating the values of M and N in this scenario as displayed in Figure (4)

$$M = \frac{\Delta t f - \Delta t \log}{\rho_b - \rho_f} \times 0.01 \quad (6)$$

$$N = \frac{\Phi N f - \Phi N \log}{\rho_b - \rho_f} \quad (7)$$

where,  $\Delta t f$  = interval transit time in oil fluid ( $\mu\text{sec}/\text{ft}$ ),  $\Delta t \log$  = interval transit time (log reading),  $\rho_b$  = log reading bulk density,  $\rho_f$  = fluid density for oil,  $\Phi N f$  = neutron porosity for fluid (oil),  $\Phi N \log$  = neutron porosity (log reading).

#### 2. Lithology (Density vs. Neutron) Cross plot

The density vs. neutron cross plot has long been used as a quantitative interpretational tool for lithology determination (Asquith and Krygowski, 2004). It can also be used to identify the gas-bearing zones, that are indicated by values above the sandstone line in the Schlumberger (1987) chart as shown in Figure (5).

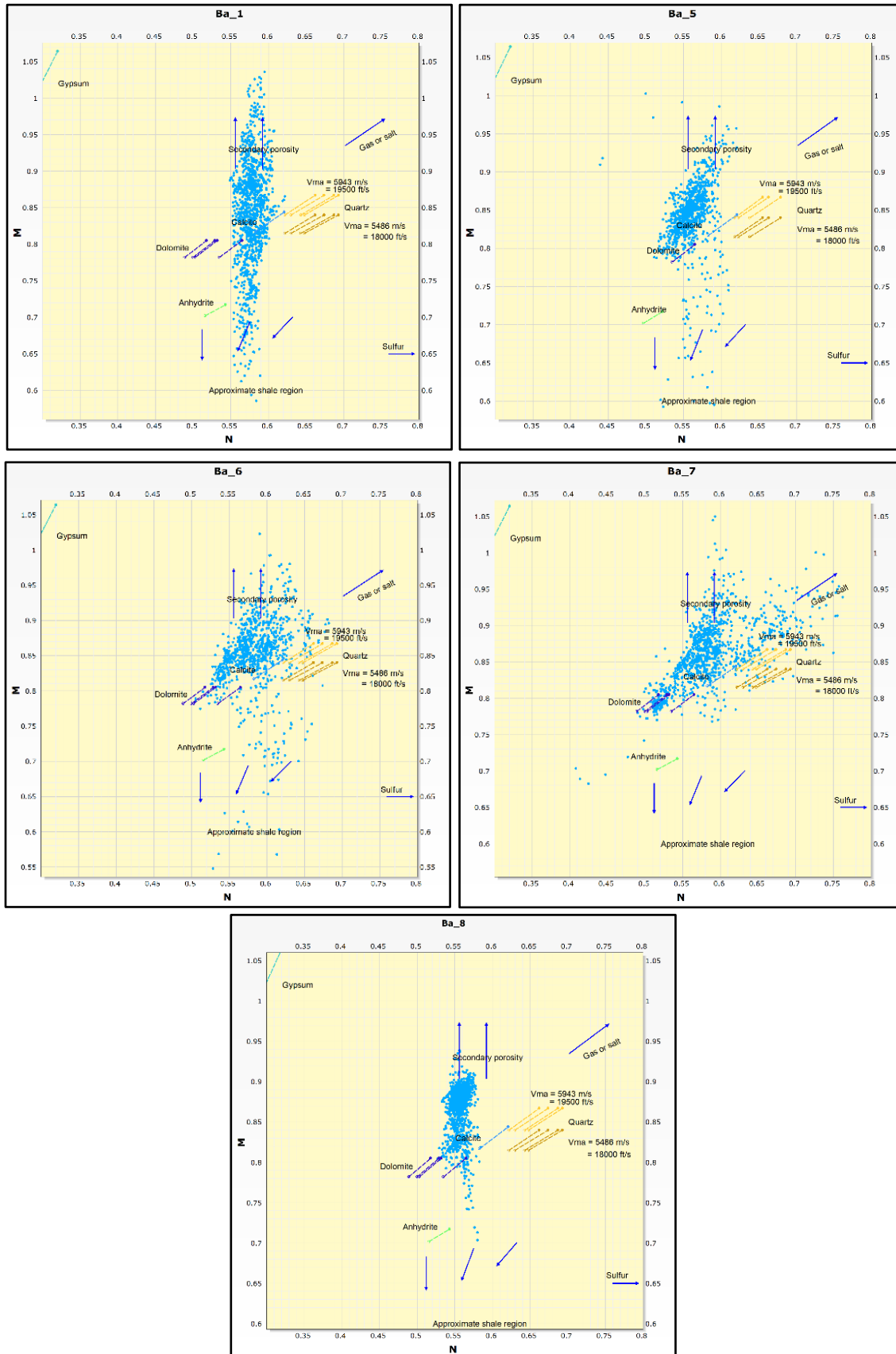


Fig. 4. M-N cross plot for five studied wells within the Hartha Formation (Schlumberger, 1979).

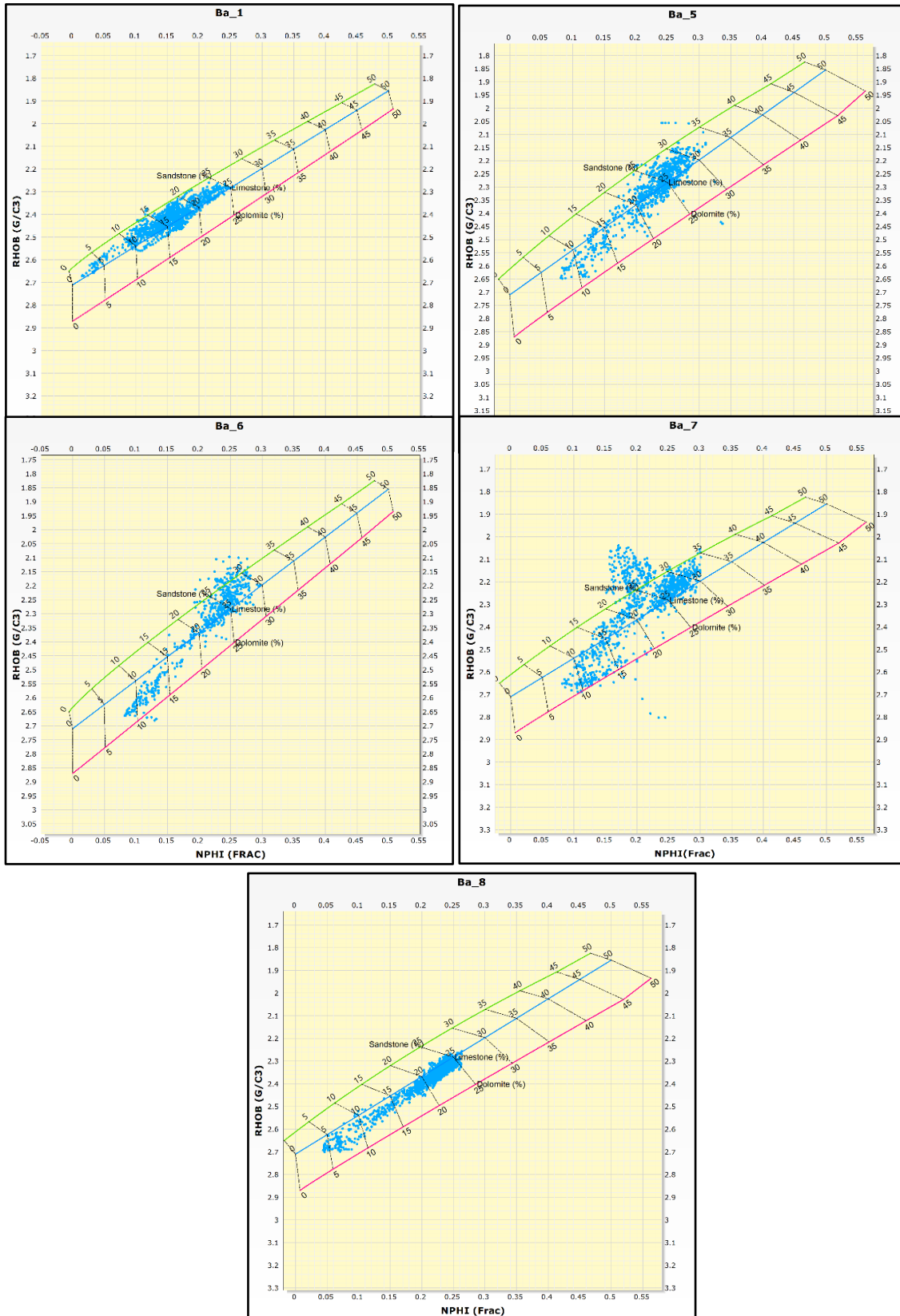


Fig. 5. Neutron versus density cross plot for five studied wells within the Hartha Formation (Schlumberger, 1987).

### Resistivity Logs

The electrical resistivity log is well-defined as the ability of the rock matrix to resist the electric current passing through its porous media. It is considered one of the most important logs that can differentiate between hydrocarbon and water-bearing formation because both the

rock's matrix and hydrocarbons are non-conductive materials (Inteq,1992). As hydrocarbon saturation increases, the rock resistivity will increase. The resistivity is measured in ohm-m and it is reciprocal to the electrical conductivity that is expressed in milliohms per meter mmohm/m (Schlumberger, 1987, 1989, 1998; Halliburton, 2001). In this study, the Laterologs logs are used to evaluate the Hartha Formation including the Microspherically Focused Log (MSFL), Shallow Laterolog (LLS), and Deep Laterolog (LLD) as shown in CPI figures (7 to 11).

### 1. Determination of Mud Filtrate Resistivity (Rmf)

To determine the water saturation in the flushed zones, the resistivity of mud filtrate is the first step that needs to be corrected at the Hartha Formation temperature. Since the (Rmf) at surface conditions can be obtained from the well header (Asquith and Krygowski, 2004) as the following formula:

$$RTF = \frac{R_{temp}(Temp+ 21)}{(Tf+ 21)} \quad (8)$$

where,  $RTF$ = the resistivity at formation temperature,  $R_{temp}$  = resistivity at surface condition,  $temp$  = temperature at which resistivity was measured,  $Tf$  = formation temperature (68)° Celsius in this study

The formation temperature (Hartha Formation temperature) at the TD can be estimated from the following formula (Arps, 1964):

$$TF= G.G *d + Ts \quad (9)$$

where,  $TF$ = formation temperature,  $G.G$  = geothermal gradient (0.015)° Celsius in this study,  $d$  = formation depth,  $Ts$  = surface temperature (30)° Celsius in this study.

### 2. Formation Water Resistivity (Rw)

Determining the resistivity of formation water is crucial for accurately calculating water saturation in the uninvaded zone (Schlumberger, 1998). There are a lot of various methods that are used to estimate the (Rw), including spontaneous potential (Sp) curves, temperature and ion concentration, and salinity versus temperature curves (Asquith and Gibson,1982). In the present study, the formation water resistivity (Rw) is determined using the total salinity versus temperature curves method. The Schlumberger (1997) chart is used for estimation, based on the chemical water analysis reports provided by the North Oil Company for the Hartha Formation. The NaCl concentration is (251,046) ppm and the Hartha Formation temperature is (68)° Celsius, so the Rw value was equal to (0.023) ohm/m.

### 3. Formation Resistivity Factor (F)

The resistivity of a rock filled with oil and/or gas within the pore spaces will be higher compared with the same rock filled with connate water in its pores (Tiab and Donaldson, 2015). Archie (1942) illustrated the relationship between the resistivity of a formation fully saturated with water (Ro), the water resistivity (Rw), and the formation resistivity factor (F) as follows:

$$Ro = F \times Rw \text{ or } F = Ro/Rw \quad (10)$$

Archie's experiments discovered that the formation factor can be linked to formation porosity as the following equation. The conventional values for carbonate rocks are (a = 1, and m 2) according to Archie (1942).

$$F = \frac{a}{\phi^m} \quad (11)$$

where, a = tortuosity factor, m = cementation factor,  $\phi$  = total porosity.

## Fluid and Bulk Volume Analysis

### 1. Water and Hydrocarbon Saturation

The water saturation, denoted by ( $S_w$ ), represents the amount of the formation water that completely occupied the pore volume of the entire rock. It can be denoted as a fraction or percentage (Inteq, 1992). The Archie equations can be utilized to determine the water saturation in both the invaded zone ( $S_{xo}$ ) and the uninvaded zone ( $S_w$ ) as shown in Figure (6), and as illustrated in the formulas below:

$$S_{xo} = (F \cdot R_{mf} / R_{xo})^{\frac{1}{n}} \quad (12)$$

$$S_w = (F \cdot R_w / R_t)^{\frac{1}{n}} \quad (13)$$

where,  $S_{xo}$  = invaded zone water saturation,  $S_w$  = uninvaded zone water saturation,  $F$  = formation factor,  $R_{mf}$  = mud filtrate resistivity at formation temperature,  $R_{xo}$  = invaded zone resistivity,  $n$ : saturation exponent (expected to be 2 for carbonate),  $R_w$  = water formation resistivity,  $R_t$  = true resistivity.

The hydrocarbon saturation represents the residual of void spaces that are not filled with water. It can be estimated from the water saturation relationships according to Schlumberger (1987) as shown in Figure (6), and as the following formula:

$$S_h = 1 - S_w \quad (14)$$

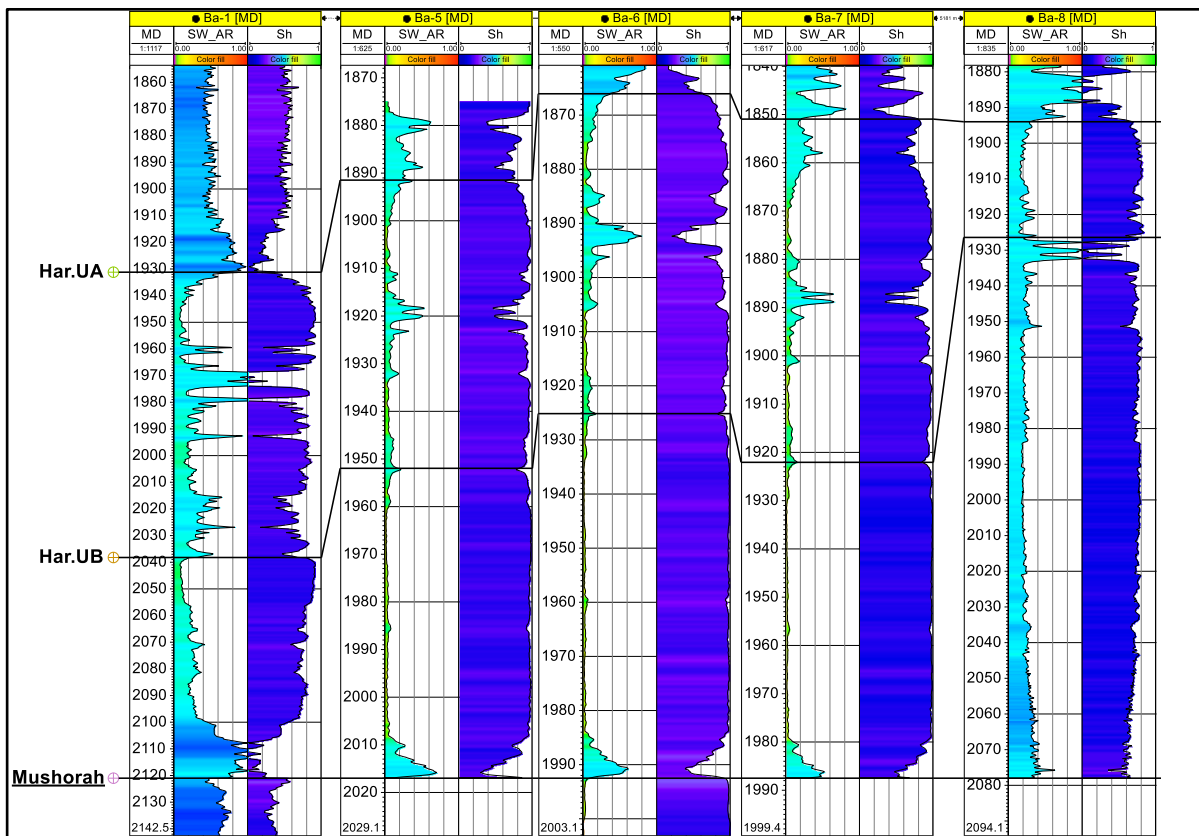


Fig. 6. The distribution of water saturation (SW) and hydrocarbon saturation (Sh) of Hartha units (A and B) for five studied wells at Balad oil field.

The water saturation in the invaded zone ( $S_{xo}$ ) and the water saturation in the uninvaded zone ( $S_w$ ) can be employed to determine the movable and residual oil saturation based on Schlumberger's (1998) equations as shown in CPI figures (7 to 11).

$$MOS = S_{xo} - S_w \quad (15)$$

$$ROS = 1 - S_{xo} \quad (16)$$

where,  $MOS$  = Movable oil saturation,  $ROS$  = Residual oil saturation

## 2. Bulk Volume Analysis

The total volume of water (BVW) in the formation can be estimated through the porosity and water saturation relationship (Asquith and Gibson, 1982). As per Schlumberger (1987), the BVW in the flushed and uninvaded zones can be determined using the following formulas, and as shown in CPI figures (7 to 11).

$$BVW = S_w * \emptyset \quad (17)$$

$$BVXO = S_{xo} * \emptyset \quad (18)$$

where,  $BVW$  = water bulk volume of uninvaded zone,  $BVXo$  = water bulk volume of invaded zone.

The total volume of hydrocarbons (movable and residual) can be estimated using the equation provided by Asquith and Krygowski (2004):

$$Bvo = Sh * \Phi \quad (19)$$

where,  $Bvo$  = hydrocarbon bulk volume,  $Sh$  = hydrocarbon saturation,  $\Phi$  = porosity

## Conclusion

The petrophysical study of the Hartha Formation shows that the (Har. UB) unit of the lower part of the formation in all the wells has good reservoir properties, where it is characterized by a high porosity and low water saturation except the (Har. UA) at the well (Ba\_1) which shows the opposite results because the thickness of this unit is very high compared with other wells.

Based on the neutron vs. density cross-plot analysis, it is evident that the lithology of the Hartha Formation primarily consists of limestone with dolomite occurring as a secondary component. Additionally, the M-N cross plot exposes that the main minerals present in the Hartha Formation are predominantly calcite, with secondary occurrences of dolomite, shale, and secondary porosity.

The wells located on the northeast block, which represents an enlarged closed fold, and contains oil and gas caps depending on the neutron and density logs separation. This separation is obvious in Ba\_6 and Ba\_7, whereas the neutron and density separation in Ba\_5 shows only oil. On the other hand, the wells located in the Graben area (Ba-1 and Ba\_8) are deeper than the northeastern wells and they contain only oil.

The diagenetic process has a significant impact on the rocks of the Hartha Formation, which has created high secondary porosity that is commonly observed in all the studied wells.

The mobile hydrocarbons in (Ba-1 and Ba-8) exhibit higher values, ranging from (0.51 to 0.65), compared to the residual hydrocarbons in Har.UA and Har. UB, which range from (0.054 to 1.02). Conversely, the movable hydrocarbons in (Ba-5, Ba-6, and Ba-7) show that the lower part of the Hartha Formation (Har. UB) displayed lower readings, ranging from (0.26 to 0.43), than the upper part of the Hartha Formation (Har. UA), which range from (0.57 to 0.72).

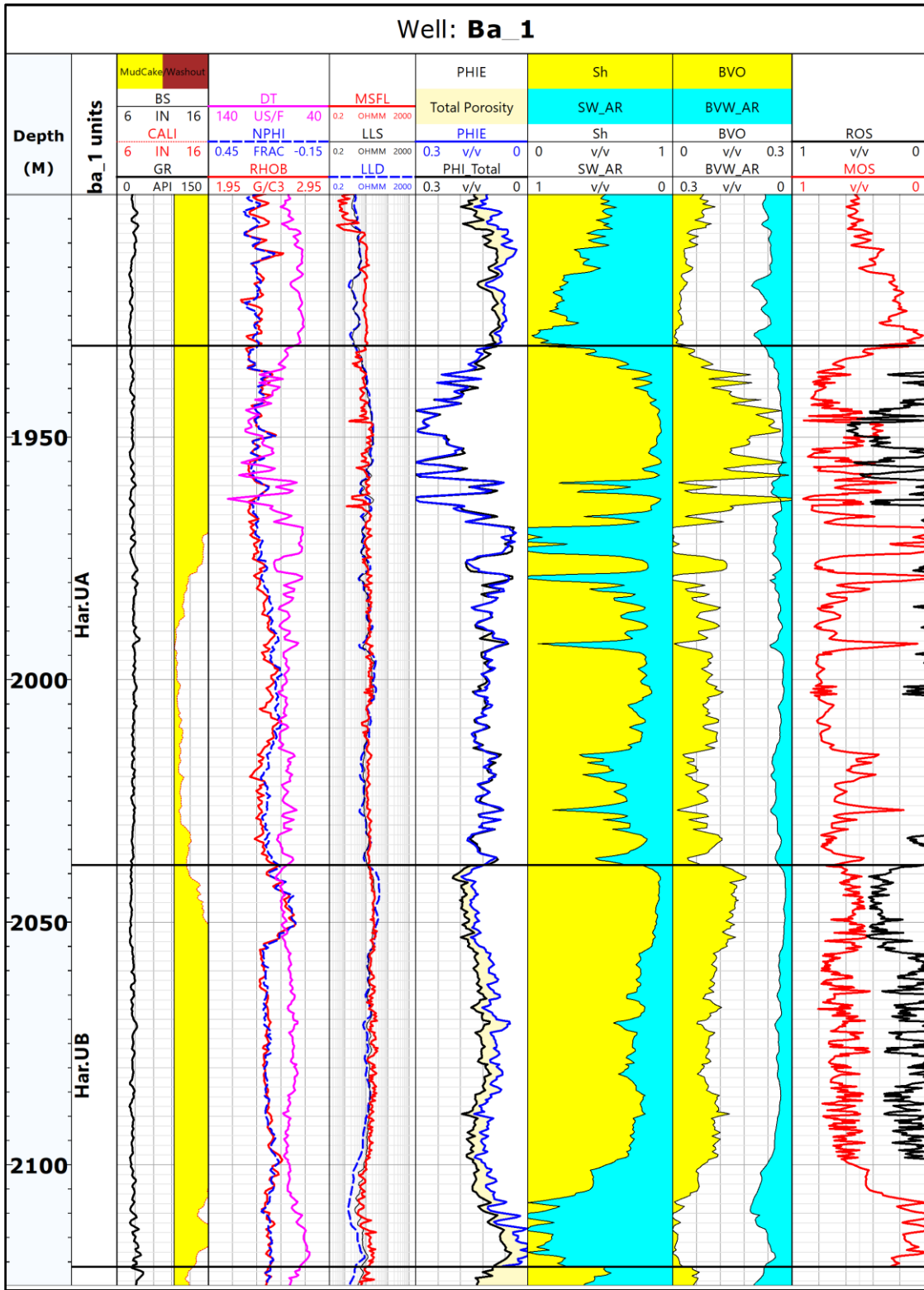


Fig. 7. The computer processing interpretation (CPI) for Ba\_1.

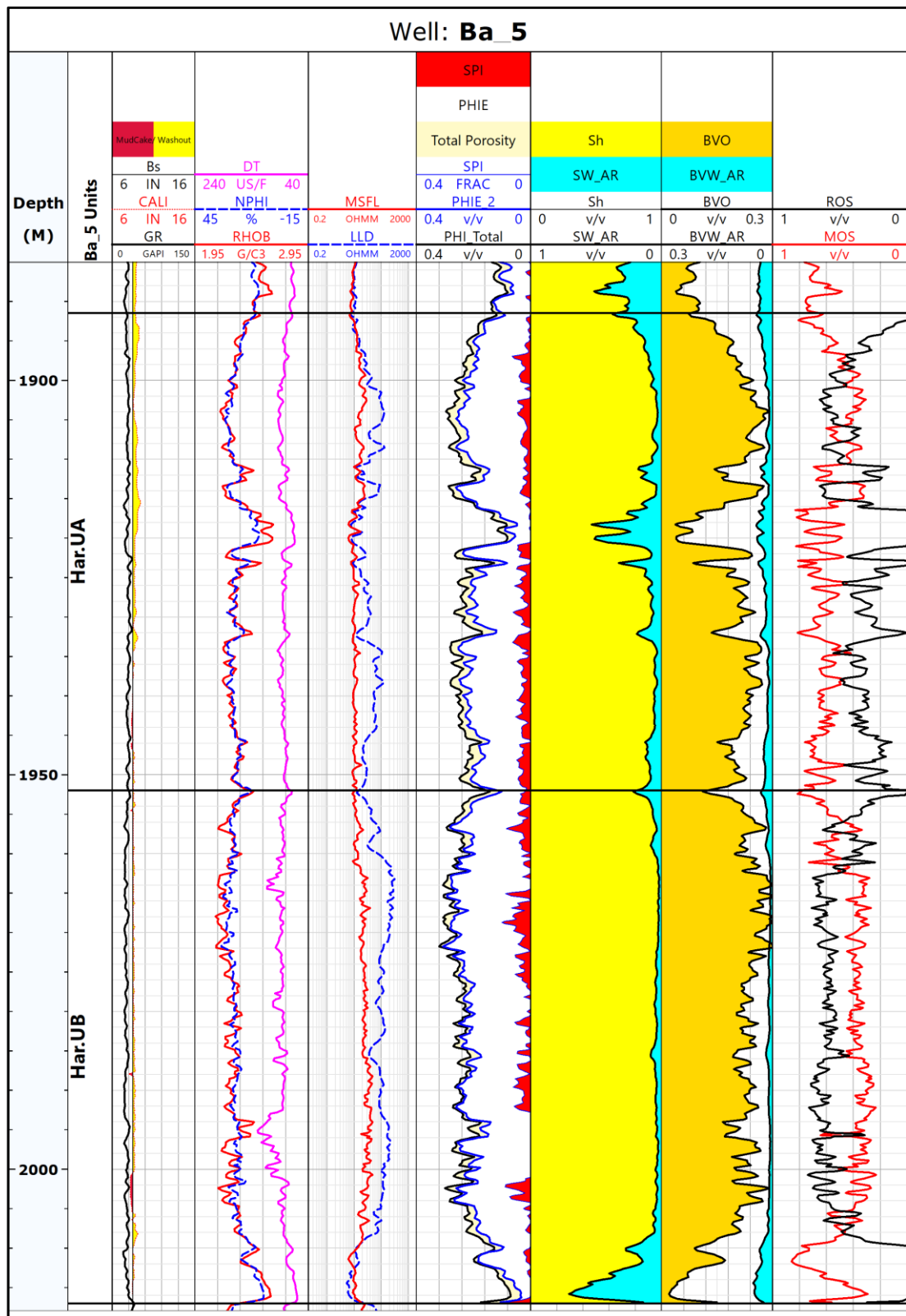


Fig. 8. The computer processing interpretation (CPI) for Ba\_5.

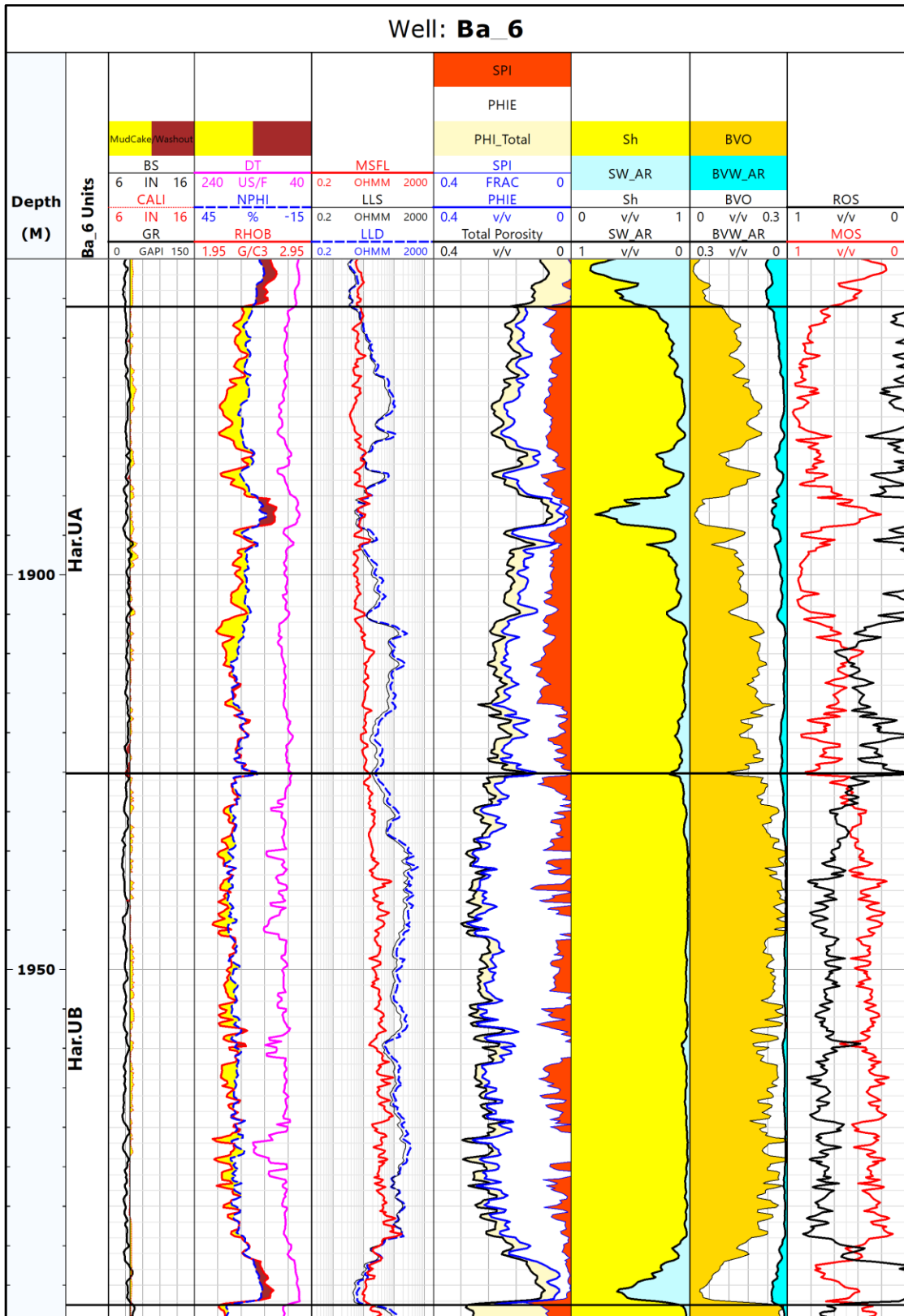


Fig. 9. The computer processing interpretation (CPI) for Ba\_6.

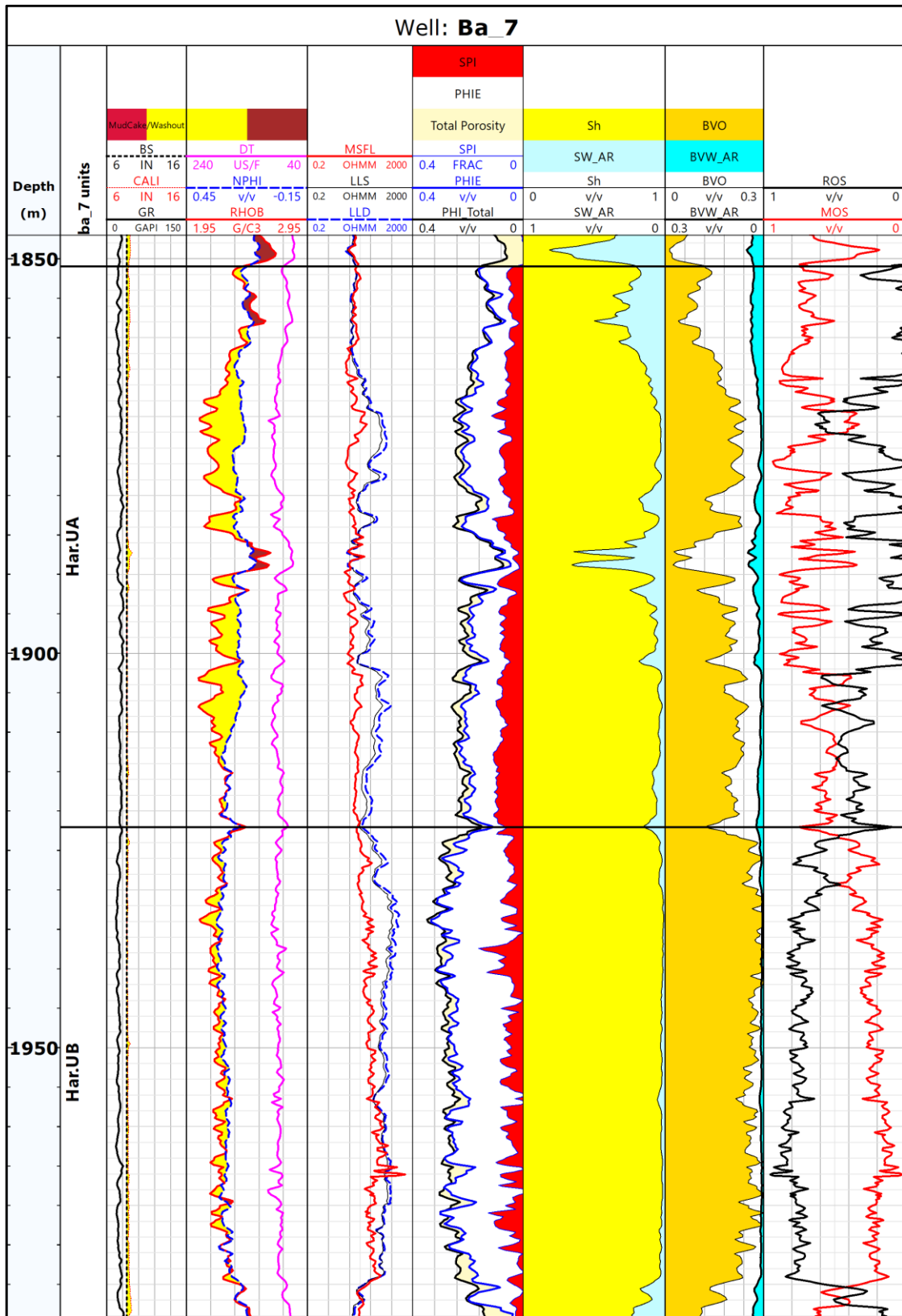


Fig. 10. The computer processing interpretation (CPI) for Ba\_7.

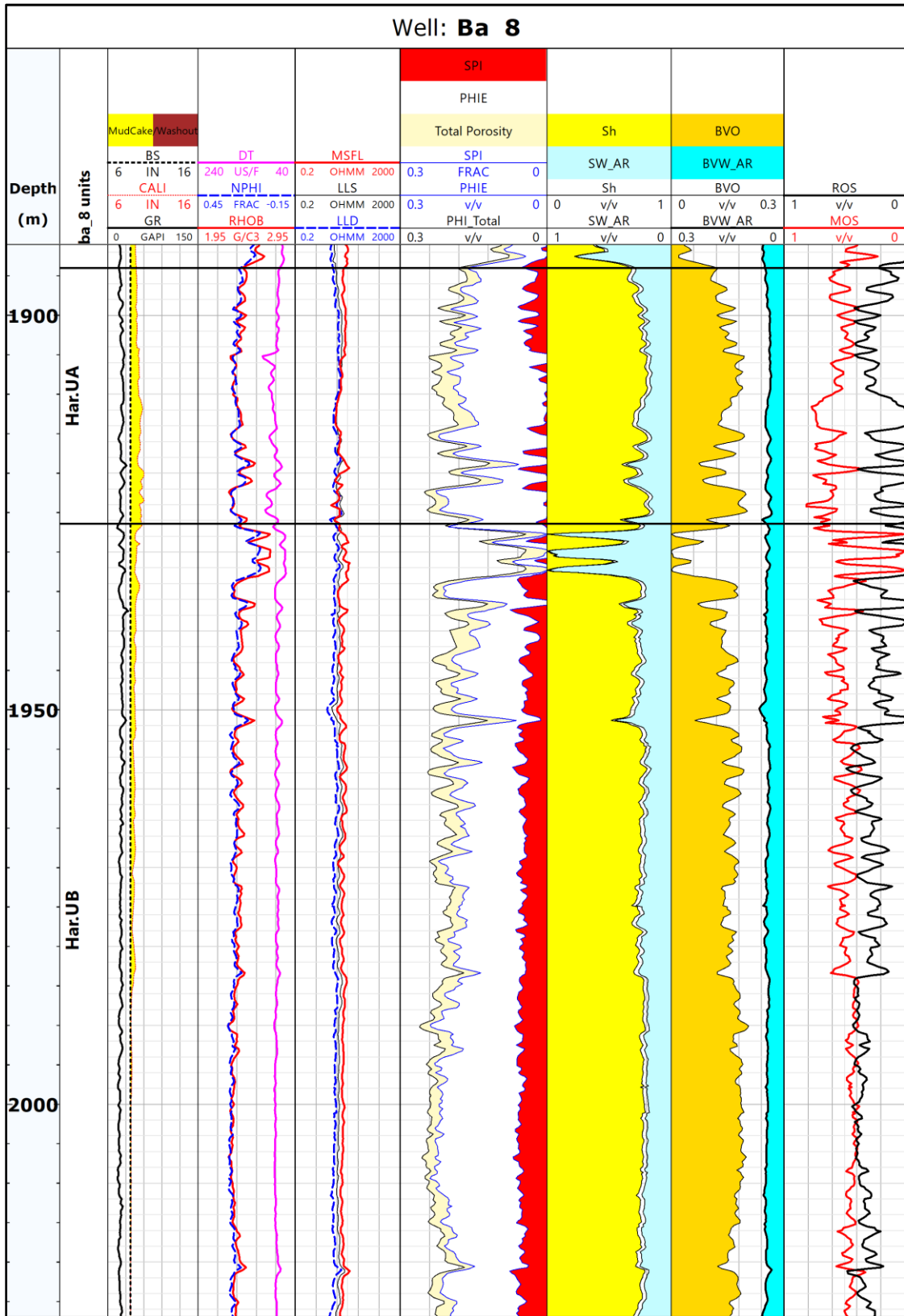


Fig. 11. The computer processing interpretation (CPI) for Ba\_8.

### Acknowledgments

We express our sincere appreciation and gratitude to the North Oil Company for generously providing the necessary data for this study. Additionally, we would like to express our thanks to the reviewers for their valuable feedback, which greatly contributed to improving the quality of this paper.

## References

- Al-Naemi, A.I., 2012. Structural Study of Balad Field and Its Reservoir Indications, Unpublished MSc. Thesis, Tikrit University, College of Science, 120 P.
- AL-Sammarai, Z.N., 2010. Hydrocarbon Prospectivity of Upper Cretaceous Formation in Balad Oil Field Salah AL-Deen Area, unpublished master's thesis, Baghdad University, College of Science, 133 P.
- Archie, G.E., 1942. The Electrical Resistivity Log as an Aid in Determining Some Reservoir Characteristics. Transactions of the AIME, 146(01), pp. 54-62. <https://doi.org/10.2118/942054-G>
- Arps, J.J., 1964. Engineering Concepts Useful in Oil Finding. AAPG Bulletin, 48(2), pp. 157-165. <https://archives.datapages.com/data/bulletns/196164/data/pg/0048/0002/0150/0157.htm>
- Asquith, G.B. and Gibson, C.R., 1982. Basic Well Log Analysis for Geologists: Methods in Exploration Series, AAPG, 216 P. <https://archives.datapages.com/data/specpubs/method16/me16ch00/me16ch00.htm>
- Asquith, G.B., Krygowski, D. and Gibson, C.R., 2004. Basic Well Log Analysis, Vol. 16, Tulsa: American Association of Petroleum Geologists. <https://doi.org/10.1306/Mth16823>
- Buday, T., 1980. The Regional Geology of Iraq: Stratigraphy and Paleogeography, Vol. 1, State Organization for Minerals, Directorate General for Geological Survey and Mineral Investigations, Al-Mosul, Iraq, 443 P.
- Buday, T. and Jassim, S., 1987. The Regional Geology of Iraq: Tectonics, Magmatism, and Metamorphism. In: Kassab, I.I. and Abbas, M.J., Eds., Geology of Iraq, Geologic Survey, Baghdad, 445 P. [https://books.google.iq/books/about/The\\_Regional\\_Geology\\_of\\_Iraq\\_Tectonism\\_m.html?id=2VxPAQAAIAAJ&redir\\_esc=y](https://books.google.iq/books/about/The_Regional_Geology_of_Iraq_Tectonism_m.html?id=2VxPAQAAIAAJ&redir_esc=y)
- Cheng, Y., Yan, C. and Han, Z., 2023. Rock Composition and Physical Properties. In Foundations of Rock Mechanics in Oil and Gas Engineering, pp. 47-69, Singapore: Springer Nature Singapore. [https://doi.org/10.1007/978-981-99-1417-3\\_3](https://doi.org/10.1007/978-981-99-1417-3_3)
- Fouad, S.F., 2010. Tectonic and Structural Evolution of the Mesopotamia Foredeep, Iraq. Iraqi Bulletin of Geology and Mining, 6(2), pp. 41-53. [https://www.researchgate.net/publication/266596604\\_Tectonic\\_and\\_structural\\_evolution\\_of\\_the\\_Mesopotamia\\_foredeep\\_Iraq](https://www.researchgate.net/publication/266596604_Tectonic_and_structural_evolution_of_the_Mesopotamia_foredeep_Iraq)
- Gadekea, L.L., Seifert, D.J. and Smith, H.D., 1988. Calibration and Analysis of Borehole and Formation Sensitivities for Gamma-Ray Spectroscopy Measurements With Multiple Radioactive Tracers. The Log Analyst, 29(03). <https://onepetro.org/petrophysics/article-abstract/171913/Calibration-And-Analysis-Of-Borehole-And-Formation>
- Halliburton, A.D., 2001. Basic Petroleum Geology and Log Analysis. Halliburton Company, 80 P.
- Haq, B.U., Hardenbol, J.A.N. and Vail, P.R., 1987. Chronology of Fluctuating sea Levels Since the Triassic. Science, 235(4793), pp. 1156-1167. DOI: [10.1126/science.235.4793.1156](https://doi.org/10.1126/science.235.4793.1156)
- Inteq, B.H., 1992. Advanced Wire line & MWD Procedures Manual. Technical Publication paper, (80459H).
- Jassim, S.Z., Goff, J.C., 2006. Geology of Iraq. Published by Dolin, Prague and Moravian Museum, Srno. 341 P.

- Lucia, F.J., Kerans, C. and Jennings Jr, J.W., 2003. Carbonate Reservoir Characterization. *Journal of Petroleum Technology*, 55(06), pp. 70-72.  
<https://doi.org/10.2118/82071-JPT>
- Numan, N.M., 1997. A Plate Tectonic Scenario for the Phanerozoic Succession in Iraq. *Iraqi Geological Journal*, 30(2), pp. 85-110.  
[https://www.researchgate.net/publication/262368041\\_A\\_plate\\_tectonic\\_scenario\\_for\\_the\\_Phanerozoic\\_succession\\_in\\_Iraq](https://www.researchgate.net/publication/262368041_A_plate_tectonic_scenario_for_the_Phanerozoic_succession_in_Iraq)
- Owen, R.M.S. and Nasr, S.N., 1958. *Stratigraphy of the Kuwait-Basra Area: Middle East*.
- Prather, B.E., Goldstein, R.H., Kopaska-Merkel, D.C., Heydari, E., Gill, K. and Minzoni, M., 2023. Dolomitization of Reservoir Rocks in the Smackover Formation, Southeastern Gulf Coast, USA. *Earth-Science Reviews*, p.104512.  
<https://doi.org/10.1016/j.earscirev.2023.104512>
- Schlumberger., 1972. *Log Interpretation, Vol. I- principles*: New York, Schlumberger Ltd., 112 P.
- Schlumberger., 1979. *Log Interpretation Charts*, Schlumberger Well Surveying Corporation, U.S.A., 97 P.
- Schlumberger., 1987. *Log interpretation charts*, USA.
- Schlumberger., 1989. *Log Interpretation Principles/ Applications*. 225 Schlumberger Drive, Sugar Land, Texas 77478.
- Schlumberger., 1997. *Log Interpretation Charts*, Houston, Schlumberger Wireline, and Testing. 193 P.
- Schlumberger., 1998. *Cased Hole Log Interpretation Principles/ Applications*, Houston, Schlumberger Wireline and Testing, 198 P.
- Selley, R.C., 1998. *Elements of Petroleum Geology*. Gulf Professional Publishing.
- Tiab, D. and Donaldson, E.C., 2015. *Petrophysics: Theory and Practice of Measuring Reservoir Rock and Fluid Transport Properties*. Gulf Professional Publishing. 239 P.  
[https://www.researchgate.net/publication/228078208\\_Petrophysics\\_Theory\\_and\\_Practice\\_of\\_Measuring\\_Reservoir\\_Rock\\_and\\_Fluid\\_Transport\\_Properties\\_Second\\_Edition](https://www.researchgate.net/publication/228078208_Petrophysics_Theory_and_Practice_of_Measuring_Reservoir_Rock_and_Fluid_Transport_Properties_Second_Edition)